Journal of Neuroradiology 46 (2019) 336–339

Available online at ScienceDirect www.sciencedirect.com

Elsevier Masson France EM|consulte www.em-consulte.com

Correspondence

Cerebral amyloidoma: A mimicker of granulomatous disease on brain MRI

Introduction

Amyloid is a pathological aggregate of insoluble fibrillary proteins either as a systemic process or limited to specific organs. Amyloid is most commonly composed of common proteins (such as serum amyloid P or mucopolysaccharide) associated with a specific protein (light chain, kappa or lambda, beta amyloid, prion, transthyretin, etc.) [1–3]. Intracranially, the most common forms of amyloid are derived from Aβ protein, which deposits inside blood vessel walls, causing cerebral amyloid angiopathy (CAA) and presenting with intracranial hemorrhage or forming the hallmark neuritic plaques of Alzheimer's disease [4]. Isolated tumefactive amyloid deposits in the brain, not related to a systemic process, are known as cerebral amyloidoma [5–7]. Other, rarer manifestations of central nervous system (CNS) amyloid are certain spongiform encephalopathies, and familial dementias [8].

Cerebral amyloidoma is a known mimicker of primary CNS neoplasms [5]. Several cases of cerebral amyloidoma have been previously reported in the literature, mostly describing a solitary mass. Hereby, we report a case of cerebral amyloidoma radiologically mimicking granulomatous diseases of the brain and involving the hypothalamus.

Description of the case

A 56-year-old man was referred for brain magnetic resonance imaging (MRI) as part of the workup for secondary (central) hypothyroidism that had been identified during evaluation for persistent fatigue. Other pituitary hormones were normal. Cerebrospinal fluid (CSF) analysis was normal, with attention to cells, protein, culture, and oligoclonal bands. Brain MRI showed several small enhancing nodules that were predominantly centered in the right hypothalamic area, with surrounding areas of T2 hyperintensity and mild mass effect on the lateral wall of the anterior third ventricle (Fig. 1). The enhancement pattern of nodules was either solid or ring-like. Some of the enhancing nodules had low T2 signal with increased ADC values. Dark signal on susceptibility-weighted images (SWI) was seen more laterally and in the medial aspect of the right lentiform nucleus. No susceptibility was identified along the deep medullary veins. The findings were initially thought to be suggestive of lymphoma versus granulomatous inflammation (such as sarcoidosis) or granulomatous infection (such as mycobacterial). PET-CT (not shown) revealed no pathologically increased FDG uptake in the head, chest, abdomen or pelvis. The computed tomography (CT) component did not reveal appreciable calcifications associated with the lesions. To determine a management strategy in the setting of a radiologic differential diagnosis including inflammatory, infectious, and neoplastic disease, a stereotactic biopsy of the right hypothalamic lesions was performed.

Intraoperatively, smear preparations showed an amorphous, clumped, eosinophilic substance (Fig. 2A). The background was of low cellularity, with only scattered macrophages and reactive gliosis. No features of a glial or hematopoietic neoplasm were seen, and no granulomatous inflammation was identified. On permanent sections (Fig. 2B-C), routine stains confirmed a component of acellular, globular, pale eosinophilic material with a periphery containing heavily calcified vessels adjacent to brain tissue with piloid gliosis. The lesion lacked a significant inflammatory cell component, other than scattered macrophages and an occasional foreign body type giant cell, and no significant plasma cell population was seen. A Congo red stain was positive in the eosinophilic material, with apple-green birefringence under polarized light microscopy (Fig. 2D). Immunohistochemical stains for kappa and lambda light chains showed strong staining of the amyloid for lambda light chains, and weak staining for kappa light chains (Fig. 2E) and transthyretin (not pictured), interpreted as nonspecific background staining. In-situ hybridization for kappa and lambda did not reveal a light chain restricted plasma cell population. Electron microscopy showed an aggregate of fibrillary material measuring 7 to 11 nm in diameter (Fig. 2F). The final pathologic diagnosis was amyloidoma, lambda light chain type. Considering the association of this pathologic process with a lymphoid or hematopoetic neoplasm, a careful hematologic follow-up was recommended.

Serum protein electrophoresis, bone marrow biopsy, and fat pad biopsy were normal. The patient received a course of dexamethasone, and follow-up MRI 13 months after the biopsy showed slightly decreased size of the lesions. The patient remains on dexamethasone therapy and under clinical and imaging surveillance.

Discussion

Central nervous system (CNS) amyloidoma is rare, but critical to recognize because clinical and radiological findings can mimic a primary glial neoplasm [9,10]. Amyloidomas have been reported in various locations of the CNS, most commonly in supratentorial parenchyma and rarely in the dura [9,11,12]. Most reported cases in the literature include a solitary circumscribed or infiltrative mass extending up to the lateral ventricular wall [6,7,9,13–17]. In some cases, finely irregular radiating lines at the edge of the tumor have been observed [6,7,14,16], thought to be a reflection of pathologically known deposition along the blood vessels [13]. In one case, cerebral amyloidoma was reported in association with intracerebral hemorrhage [18].

The reported MRI characteristics of amyloidoma are variable. On T1-weighted images, it can be hypointense [9,16], isointense [7], or hyperintense [6]. T2 signal intensity is usually mixed, including nodules of low signal intensity mixed with regions of higher signal likely due to non-uniform deposition of amyloid [5]. Post-contrast

https://doi.org/10.1016/j.neurad.2019.02.009

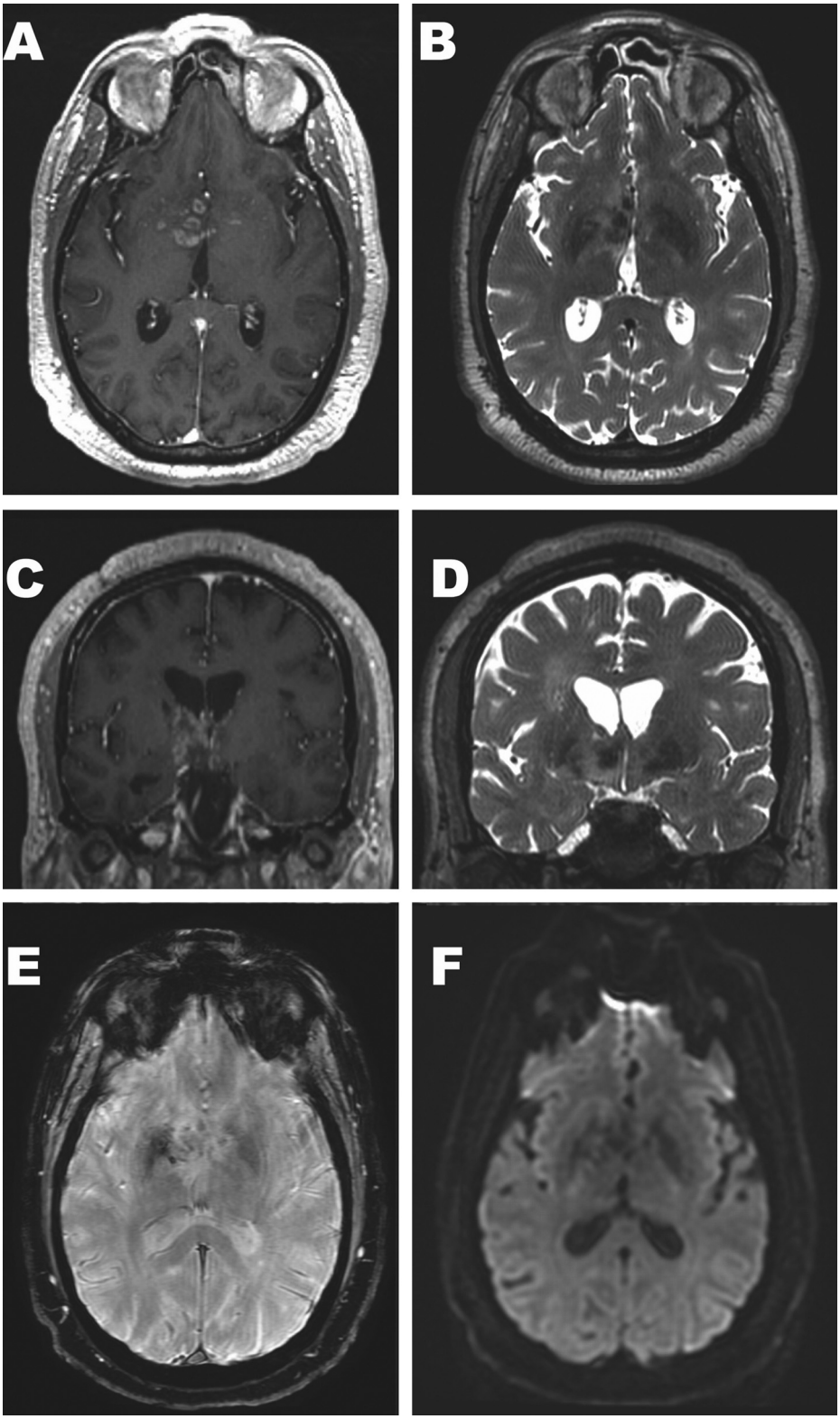

Fig. 1. Axial post-contrast T1-weighted (A), Axial T2-weighted (B), coronal post-contrast T1-weighted (C), and coronal T2-weighted (D) images demonstrate several small peripherally or solidly enhancing nodules with areas of low T2 signal clustered in the region of the right hypothalamus and to a lesser extent in the right ventral thalamus and left hypothalamus. There is mild mass effect on the right aspect of the anterior third ventricle. Axial susceptibility-weighted image (E) shows asymmetric susceptibility in the region of medial right lentiform nucleus corresponding to tiny enhancing vessels in the same area on post-contrast axial image (A). Small vessels in this area were heavily calcified on pathology. Diffusion-weighted image (F) shows no areas of reduced diffusion.

T1-weighted images usually show faint or intense enhancement [9]. It has been speculated that peripheral contrast enhancement could be related to amyloid deposition in blood vessel walls and disruption of blood brain barrier [5]. We observed areas of dark signal on SWI, which may be related to hemorrhage and blood products [18], or presence of calcifications along small blood vessels (as was

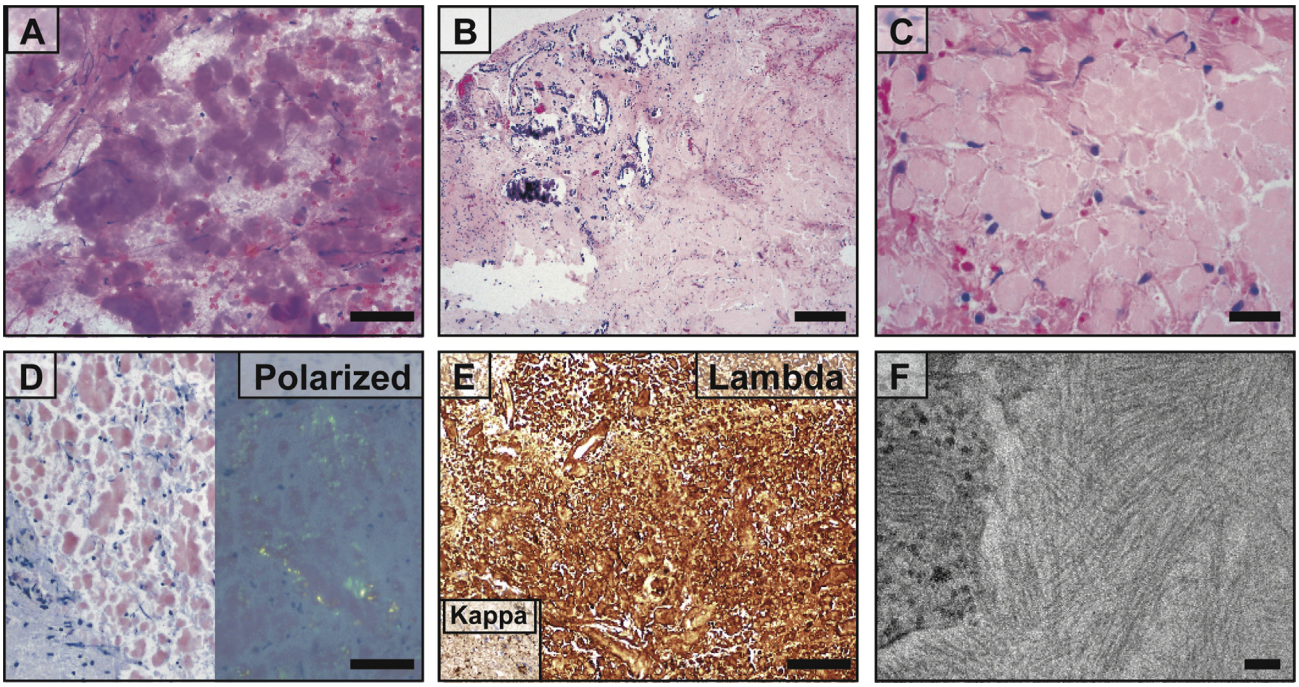

Fig. 2. (A) Hematoxylin and eosin (H&E) stained Intraoperative smear preparations showed an amorphous eosinophilic substance, on a background of low cellularity and reactive gliosis. Scale bar = 50 μm (B-C) Permanent sections demonstrated gliosis and aggregates of acellular wax-like eosinophilic material, with scattered inflammatory cells and heavily calcified small vessels. Scale bars = 200 μm and 50 μm for B and C, respectively. (D) Staining with Congo red is positive (left panel) and shows apple-green birefringence when visualized under polarized light (right panel). Scale bar = 50 μm. (E) The amorphous deposits are strongly positive with immunohistochemistry for lambda light chain, while kappa light chain (inset) shows only weak staining. Scale bar = 100 μm. (F) Ultrastructural examination by electron microscopy shows abundant deposition of fibrillary material ranging from 7 to 11 nm in diameter. Scale bar = 50 nm.

seen on pathologic specimens in this case). These microcalcifications may not be dense enough to be visible on brain CT considering limitations in image resolution. Cerebral catheter angiography (if performed) is normal or shows displacement of vessels due to mass effect from amyloidoma. Our case had a different imaging appearance consisting of several peripherally or solidly enhancing nodules around the third ventricle. The imaging appearance was initially thought to be suggestive of lymphoma, or a granulomatous process with a likely perivascular distribution. However, the biopsy findings were definitive for amyloidoma. To the best of our knowledge, no previous case with such imaging features has been reported in the literature.

Most cerebral amyloidomas are of the light chain (AL) lambda-restricted type [1,2,11,19]. In a recent series that included seven patients with primary CNS amyloidoma, Hess et al found evidence of a monoclonal B-cell population in all cases [2], agreeing with previous reports of an association between CNS amyloidoma and low-grade B-cell neoplasia [11,20]. In this report, we identified a lambda-restricted amyloidoma, but no underlying evidence of a clonal lymphoid population. Systemic evaluation for lymphoma or myeloma in this patient was negative. Yet, we cannot entirely exclude the possibility of undersampling of the CNS lesion.

Overall, CNS amyloidoma is usually associated with a stable clinical course and favorable prognosis. However, the small number of reported CNS cases makes treatment decisions challenging, and the association with a clonal B-cell population and potential progression to systemic amyloidosis supports careful clinical follow-up [1,2,20,21].

Disclosure of interest

The authors declare that they have no competing interest.

References

[1] Fischer B, Palkovic S, Rickert C, Weckesser M, Wassmann H. Cerebral AL lambda-amyloidoma: clinical and pathomorphological characteristics. Review of the literature and of a patient. Amyloid 2007;14(1):11–9.
[2] Hess K, Purrucker J, Hegenbart U, et al. Cerebral amyloidoma is characterized by B-cell clonality and a stable clinical course. Brain Pathol 2017.
[3] Wechalekar AD, Gillmore JD, Hawkins PN. Systemic amyloidosis. Lancet (London, England) 2016;387(10038):2641–54.
[4] Miller-Thomas MM, Sipe AL, Benzinger TL, McConathy J, Connolly S, Schwetye KE. Multimodality review of amyloid-related diseases of the central nervous system. Radiographics 2016;36(4):1147–63.
[5] Gallucci M, Caulo M, Splendiani A, Russo R, Ricci A, Galzio R. Neuroradiological findings in two cases of isolated amyloidoma of the central nervous system. Neuroradiology 2002;44(4):333–7.
[6] Lee J, Krol G, Rosenblum M. Primary amyloidoma of the brain: CT and MR presentation. AJNR Am J Neuroradiol 1995;16(4):712–4.
[7] Caerts B, Mol V, Sainte T, Wilms G, Van den Bergh V, Stessens L. CT and MRI of amyloidoma of the CNS. Eur Radiol 1997;7(4):474–6.
[8] Rostagno A, Holton JL, Lashley T, Revesz T, Ghiso J. Cerebral amyloidosis: amyloid subunits, mutants and phenotypes. Cell Mol Life Sci 2010;67(4):581–600.
[9] Gandhi D, Wee R, Goyal M. CT and MR imaging of intracerebral amyloidoma: case report and review of the literature. AJNR Am Journal Neuroradiol 2003;24(3):519–22.
[10] Landau D, Avgeropoulos N, Ma J. Cerebral amyloidoma mimicking intracranial tumor: a case report. Journal of medical case reports 2010;4:308.
[11] Laeng RH, Altermatt HJ, Scheithauer BW, Zimmermann DR. Amyloidomas of the nervous system: a monoclonal B-cell disorder with monotypic amyloid light chain lambda amyloid production. Cancer 1998;82(2):362–74.
[12] Shibao S, Dalpra FA, Andrade CS, Leite CC. Dural amyloidoma: An unusual presentation of CNS amyloidosis. Neurology 2016;86(13):1266–7.
[13] Eriksson L, Sletten K, Benson L, Westermark P. Tumour-like localized amyloid of the brain is derived from immunoglobulin light chain. Scand J Immunol 1993;37(6):623–6.
[14] Spaar FW, Goebel HH, Volles E, Wickboldt J. Tumor-like amyloid formation (amyloidoma) in the brain. J Neurol 1981;224(3):171–82.
[15] Moreno AJ, Brown JM, Brown TJ, Graham GD, Yedinak MA. Scintigraphic findings in a primary cerebral amyloidoma. Clin Nucl Med 1983;8(11):528–30.
[16] Cohen M, Lanska D, Roessmann U, et al. Amyloidoma of the CNS. I. Clinical and pathologic study. Neurology 1992;42(10):2019–23.
[17] Blattler T, Siegel AM, Jochum W, Aguzzi A, Hess K. Primary cerebral amyloidoma. Neurology 2001;56(6):777.
[18] Labro H, Al-Kadhimi Z, Djmil M, Oghlakian R, Alshekhlee A. Brain amyloidoma with cerebral hemorrhage. J Am Osteopath Assoc 2009;109(7):372–5.

[19] Yu JP Wilson DM, Chang EF, et al. Isolated intracerebral light chain deposition disease: novel imaging and pathologic findings. Clinical imaging 2014;38(6):868–71.
[20] Pace AA, Lownes SE, Shivane A, Hilton DA, Weatherby SJ. A tale of the unexpected: Amyloidoma associated with intracerebral lymphoplasmacytic lymphoma. J Neurol Sci 2015;359(1-2):404–8.
[21] Mahmood S, Bridoux F, Venner CP, et al. Natural history and outcomes in localised immunoglobulin light-chain amyloidosis: a long-term observational study. The Lancet Haematology 2015;2(6):e241–50.

Alireza Radmanesh [a,*]
Matthew D. Wood [b]
Andrew W. Bollen [c]
[a] *New York University School of Medicine, Department of Radiology, Division of Neuroradiology, New York, NY 10016 USA*
[b] *Oregon Health and Science University, Department of Pathology, Portland, OR 97239 USA*
[c] *University of California San Francisco, Department of Pathology, Division of Neuropathology, San Francisco, CA 94143 USA*

* Corresponding author at: 660, First avenue, 2nd Floor, New York, NY 10016, USA
E-mail address: alireza.radmanesh@nyumc.org (A. Radmanesh)

Available online 7 March 2019